Mapping the dimerization specificity of bZIP transcription factors in bread wheat

Raminder Kaur[1,2], Nishtha Sharma[1], Prateek Jain[1], Mamta Verma[1,3],

Ashish Apkari[1,2], Vikas Rishi[1]*

[1]National Agri-Food Biotechnology Institute, Knowledge City, Sector 81,

Mohali, Punjab 140306, India.

[2]Department of Biotechnology, Panjab University,

Chandigarh 160014, India.

[3]Regional Centre for Biotechnology, Faridabad,

Haryana, 160014, India.

*Corresponding author: Email: vikasrishi@nabi.res.in

Alternate email: vrishi09@gmail.com

Website: www.nabi.res.in

Abstract

Dimerization plays a pivotal role in target-binding interactions among various transcription factors (TFs), including bZIPs, bHLHs, MYBs, and zinc finger TFs. The bZIP family is defined by an α-helix class of TFs containing a basic region that binds to the major groove of double-stranded DNA (dsDNA), followed by a leucine zipper motif that mediates dimerization through coiled-coil structures, forming homo- or heterodimers. In polyploid bread wheat (*Triticum aestivum* cv.), bZIPs and their homeologs interact through the dimerization motifs to form specific bZIP pairs with distinct regulatory functions. The dimerization pattern of bZIPs is critical for gene regulation, however, the mechanisms underlying their specificity remain poorly understood. Here, we focus on the dimerization specificity of coiled-coil α- helical bZIP proteins in bread wheat, highlighting the leucine zipper region as a key dimerization motif. We identified 265 bZIPs containing the bZIP motif, following dimerization criteria established in humans, *Drosophila*, and *Arabidopsis* based on the presence of specific amino acids at the 'a', 'd', 'e', and 'g' positions in heptads. Eight key bZIP TFs were cloned, expressed, and purified for the structural analysis. This study not only provides the dimerization trend exhibited by bZIPs during thermal stability analysis but also provides the reversibility pattern followed by the thermal denaturation exposure at 85˚C. Our study also points towards that how amino acid substitutions and the length of the leucine zipper influence the formation of coiled-coil structures among bZIP homeologs of polyploid wheat. Overall, the study advances our understanding of the role of leucine zippers, in determining the specificity and stability of bZIP dimers, which in turn governs DNA binding and gene regulation in plants.

Keywords

bZIP transcription factors, Leucine zipper, Dimerization specificity, Coiled-coil structures, Bread wheat (Triticum aestivum), Thermal stability, DNA binding, Gene regulation.

1. Introduction

1.1. bZIP Transcription factors (TFs)

bZIP TFs serve as the primary mediator of environmental signals that ultimately result in gene expression. DNA-binding class of TFs interact with transcription factor complex to recruit or block the access of RNA polymerase to the promoter region of the gene, and hence trigger the gene regulation process (Krylov *et al.* 1998). Several regulatory DNA-binding transcription factors are classified based on the DNA-binding domains recognized by them such as bZIPs, bHLHs, MYBs, NACs, etc (Riechmann and Ratcliffe 2000). Many DNA binding proteins employ dimerization as an essential feature for target-binding interactions (Baxevanis and Vinson 1993).

The term bZIP comes from the basic amino acid-rich N-terminal region and the C-terminal region containing amphipathic amino acids (Krylov *et al.* 1998). Although a few bZIPs have been well characterized, the majority of the bZIP family members remain to be further explored. bZIPs are crucial

62 for various aspects of plant development and defense (Jakoby *et al.* 2002). The bZIP proteins contain a
63 continuous α-helix, including the basic region, which is essential for binding to the major groove of
64 double-stranded DNA. This is followed by the C-terminal leucine zipper motif, which facilitates
65 dimerization through a coiled-coil structure (Acharya *et al.* 2002). In bZIPs, the leucine zipper motif
66 plays a crucial role in the functional activity of various transcriptional regulatory proteins, particularly
67 in dimerization (Moitra *et al.* 1997). bZIPs bind to specific sequences of DNA. Plant bZIP transcription
68 factors like to bind to the common ACGT component sequences A-box (TACGTA), C-box (GACGTC),
69 and G-box (CACGTG) (Foster *et al.* 1994). In addition, they have been reported to bind to non-core
70 ACGT DNA motifs (Foster *et al.* 1994; Kusano *et al.* 1995).

71 Researchers initially divided the members of the bZIP TF family in *Arabidopsis* into ten groups
72 based on common domains (Jakoby *et al.* 2002). Further, the bZIPs were classified into 13 groups (A-
73 M) (Dröge-Laser *et al.* 2018). Vinson and co-workers divided the Arabidopsis bZIPs into different
74 groups based on their predicted dimerization properties (Deppmann *et al.* 2004). However, a
75 comprehensive classification of plant bZIPs based on dimerization specificity remains lacking,
76 especially in complex plant genomes like bread wheat (Triticum aestivum).

77 **1.2 Structural signatures determining the dimerization specificity in bZIPs**

78 Dimerization has emerged as an integrated property manifested by DNA binding proteins (Vinson
79 *et al.* 1989; Pathak and Sigler 1992). Dimerization involves the potential for the monomers to form
80 dimers with the associated mechanisms, which enhances their function for the incremental biological
81 control (Amoutzias et al., 2006, 2008). Newman and Keating have shown that, in Humans and Yeast,
82 about 15% of all possible interactions occur among bZIP protein (Newman and Keating 2003).

83 The bZIP structure comprises 60–80 amino acids, including an N-terminal basic DNA
84 binding region and a C-terminal adjacent leucine zipper region (Ellenberger *et al.* 1992; Deppmann
85 *et al.* 2004). The DNA binding region is abundant with basic amino acids and has a conscious N-X_7-
86 R/K motif in its DNA-binding sequence (Landschulz *et al.* 1988). The bZIP monomer comprises a
87 structural repeat of amino acids (Krylov *et al.* 1994). Each structural repeat is termed a heptad
88 consisting of seven residues designated with alphabets (*a,b,c,d,e,f*, and *g)*(Acharya *et al.* 2002;
89 Vinson *et al.* 2006). The 'a', 'd', 'e' and 'g' are prime positions in the leucine zipper interface and
90 are responsible for the dimerization stability and specificity (Acharya *et al.* 2002, 2006; Deppmann
91 *et al.* 2004; Vinson *et al.* 2006).

92 The amino acid residues at '*a*' and '*d*' positions form the hydrophobic interface on the similar
93 edge of the α-helix (Pathak and Sigler 1992). These residues interact inter-helically and stabilize the
94 structural dimer (Vinson *et al.* 2002, 2006). Leucine is frequently present in the '*d*' position and
95 stabilizes the dimer more effectively than other amino acids (Moitra *et al.* 1997). In this

configuration, the hydrophobic core formed between the non-polar surfaces of two leucine zippers causes them to dimerize (Vinson *et al.* 2002, 2006; Deppmann *et al.* 2006).

Electrostatic interactions are generated by the charged amino acids at the 'g' and 'e' positions in a heptad (Krylov et al. 1994). The ‘g’ and ‘e’ interactions are indicated as g ↔ e ′ where the prime (′) indicates a residue on the second interacting α-helix of the dimeric leucine zipper. g-e ′ interactions between oppositely charged residues encourage homodimerization (Deppmann et al. 2004). The g-e ′ interactions between likely charged residues are repulsive and encourage heterodimerization. In plant bZIPs, similar positioning of crucial amino acids is observed as in humans. Asparagine occurs at ‘*a*’ position in the second heptad of all human bZIPs, which results in homodimerization typically (Jakoby *et al.* 2002). In humans, 32% of Asparagine occurs in the second heptad at the ‘*a*’ position, whereas it is about 68% in *T. aestivum* in the present study.

The leucine zipper region comprises hydrophobic amino acids such as leucine, isoleucine, and valine (Vinson *et al.* 1989). It has also been noted that distinct heptads vary substantially in length, and the influence these length differences have, on the functional features, is a topic of active research. Understanding these structural determinants is critical for predicting bZIP dimerization behavior, particularly in complex plant genomes like wheat, where expanded bZIP families may contribute to diverse regulatory pathways. Heterodimerization is common in mammalian systems, where bZIPs like the Jun family interact with FOS members to form oncogenic complexes (Vinson *et al.* 2002). No similar system is reported in plants. To address this gap, we looked at the ability of the bread wheat bZIP sequences to form homo- or heterodimers, which may help to uncover DNA sequences that these bZIPs recognize and, by logical extension, novel genes that they may regulate.

2. Materials and methods

2.1. Plant materials

Bread wheat (Triticum aestivum) variety Chinese Spring (CS) cultivar (cv.) was grown in the experimental fields of the BRIC-National Agri-Food and Biomanufacturing Institute, Punjab, India. First day after anthesis (DAA) was considered when anthers appeared from the central portion of the spike. After the anthesis appeared, the plants were tagged for sampling at different stages of seed development such as 0,7,14,21 and 28 days after anthesis (DAA). Seed samples from spikes at different developmental stages i.e. at 7, 14, 21 and 28 DAA which corresponds to stage Z-72, Z-75, Z-78, Z-82, respectively, according to Zadoke scale were collected and stored at -80°C (ZADOKS *et al.* 1974). Tissue samples such as leaf, flag leaf, stem and root were also collected, frozen in liquid nitrogen (N_2) and stored at -80°C until further use.

2.2. Cloning of bread wheat bZIPs

For the zipper region of candidate bZIP genes, the primers were designed for the cloning experiments.

Different parameters were considered including Tm, GC content, and hairpin loop structure using Oligo Calc tool. Zipper- region of bZIPs were amplified as BamHI-HindIII fragment using Taq DNA polymerase. Quality of PCR products was checked on 1.2% agarose gel. For ligation of amplified bZIPs into pT5 protein expression vector, conventional cloning was used. All cloned fragments have T7 tag in their N–terminus region. Positive clones from pT5 vector were confirmed by Sanger-dideoxy sequencing and were attempted for sub-cloning in expression vector pET23b+. The expression vector was considered because of higher expression of bacterial recombinant proteins. Details are described in supplementary material S1 file for the methodology of recombinant protein expression, downstream processing, purification and quantification.

2.3. Multiple alignment for prediction of dimerization specificity:

Eight different TabZIPs (Embp1, TabZIP1, TaABI5 well reported in earlier studies and TraesCS4B02G320400, TraesCS5A02G237200, TraesCS7A02G398400, TraesCS1A02G072600 and TraesCS7D02G518100 as novel bZIPs) from hexaploid wheat were selected on the basis of their expression which have potential role in seed maturation and abiotic stress. Amino acids sequences of seed-specific bZIPs were aligned using the multalin sequence alignment tool. The presence of an invariant asparagine (**N**) residue in basic region of bZIPs was used for alignment of protein sequences. The N-terminal boundary for bZIP is conserved due to presence of basic amino acids while to establish C-terminal boundary, following four criteria were used: **(i)** Presence of Proline (P) or **(ii)** two constitutive Glycines (G), that disrupts α–helical structure **(iii)** repetition of leucine at 'd' position in leucine zipper and **(IV)** Presence of charged amino acids at 'e' and 'g' position (Deppmann et al., 2004). After alignment, the N–terminal and C–terminal boundaries were defined and amino acids responsible for dimerization were color coded according to previously published work (Fassler et al., 2002; Vinson et al., 2002; Deppmann et al., 2004).

2.4. Protein secondary structure analysis using Circular Dichroism

For CD, all eight protein samples used, were of highest purity. The presence of any insoluble aggregates can distort the shape and magnitude of CD spectrum that will decrease the signal/noise ratio (Kelly *et al.* 2005). For wavelength and thermal denaturation studies experiments were performed in standard CD buffer (12.5mM KPO_4 buffer pH 7.4, 150 mM KCl and 1M DTT). All circular dichroic studies were carried out using Biologic CD spectrometer (Biologic, France). Before CD studies, samples were heated to 65° C for 15 min and allowed to cool at room temperature. For structural studies, 2 mM (dimer) proteins were used. Wavelength scans of proteins were carried at 6° C and samples were scanned from 200-260 nm. Average of 5 scans for each protein sample was taken. For thermal denaturation studies protein samples were heated from 6-85˚C at the rate

of 1° C/min while change in ellipticity was measured at 222 nm. All TabZIP proteins melted with the well-defined sigmoidal transition curves. All such curves were fitted according to (equation 1) assuming denaturation to be a two-state type.

$$-\theta_{222}(T) = (N - D)\,(1 - T/T_{inter})\,[1 + 1 - (8exp\,(\Delta Hm\,(1/T_m - 1/T)/\,R + 1))1/2\,/4exp\,\Delta Hm\,(1/Tm - 1/T)/\,R] + D \qquad \text{(Equation 1)}$$

where -θ222 (T) were CD signals in millidegree (mdeg) at 222 nm at any temperature T in ° C, N is the ellipticity of the α-helical coiled coil dimer at 0° C extrapolated from the linear-dependencies of CD signals at low temperature range defined as pre-transition region, D is the ellipticity at high temperature extrapolated to 0˚ C and referred to as post-transition baseline where dimeric protein molecules melt to unhelical monomers. Transition region between pre-and post-transition region has monomer and dimer bZIPs in equilibrium. T inter is the temperature at which the linear temperature-dependencies of dimer and monomer molecules intersect, and Ris the gas constant. Fitting of thermal denaturation curves gave values of midpoint of thermal denaturation (Tm), and enthalpy change at Tm (ΔHm). Constant-pressure heat capacity change (ΔCp) was calculated using Tm versus ΔHm plot for all the possible bZIP dimers. A linear fitting of these data points with negative slope gave the value of ΔCp. This along with Tm, and ΔHm values were used to calculate ΔGDi, Gibbs free energy of dimerization at 25˚ C for each dimer by using the following form of Gibbs Helmholtz equation (Equation 2).

$$\Delta GDi = RTolnC + \Delta Hm\,[(1 - To/Tm) - \Delta Cp\,[(Tm - To) + Toln\,(To/Tm)] \qquad \text{(Equation2)}$$

where *To* is any temperature in ° C and C is total protein concentration.

2.5. Identification of amino acid variations and leucine zipper length

Being a polyploid plant, bread wheat TabZIPs were aligned (Supplementary figure 1). While aligning the sequences of the TabZIPs, some were identified as exceptionally longer and with one or more amino acid variations within the homeolog copies. TraesCS4B02G320400, TraesCS5A02G237200 out of eight TabZips, were chosen for the biochemical characterization devoted by their structural features. Presence of specific amino acids, owing to the distinct structural properties is leading to the stable helical structure formation in the bZIPs. Identification further led the basis to analyse their α-helical structure characterization and thermal stability behavior using CD spectroscopy.

2.6. **MALDI-TOF-MS protein profiling**

10 mg of sinapinic acid (SA) stock was mixed with the sample in equimolar ratio and was dried on a microtiter plate format 384 well target made out of full metal (MTP) plate. The dried layer was analyzed by a ABSCIEX TOF/TOF 5800 MALDI instrument in the mid-mass linear positive mode.

One microliter of the sample/matrix solution was spotted onto the MALDI target plate MTP 384 and left to crystallize at room temperature. All protein samples were analyzed in a random order to minimize variability and systematic errors. ABSCIEX TOF/TOF 5800 MALDI-TOF mass spectrometer (SCIEX, USA) was used to perform MS analyses in the mid mass linear positive mode. Positively charged ions were detected in the m/z range of 9000–27,000 Da and 1000 shots were accumulated per one spectrum. The MS spectra were externally calibrated using the mixture of following Sigma protein calibration standards such as ProteoMass™ Bradykinin Fragment 1-7, ACTH Fragment 18-39, Insulin chain B oxidized, Angiotensin II, Insulin, $P_{14}R$ etc. at the ratio of 1:5.

The average mass deviation was less than 100 ppm. The matrix suppression mass cut off was m/z 700 Da. The following ion source parameters were used: ion source 1, 25.09 kV; ion source 2, 23.80 kV. Other settings for MALDI-TOF MS analysis were as follows: pulsed ion extraction, 260 ns and lens, 6.40 kV. In-built software TOF-TOF series explorer software (Ab Sciex, U.S.A) was applied for the acquisition and processing of the spectra. Each sample was analyzed in three repetitions. Inter-day and intra-day reproducibility of the applied procedure was evaluated in our study.

3. Results:

3.1. Chromosomal localization of bZIP transcription factors of bread wheat

All the TabZIPs were attempted for the localization on the chromosomes covering around 91% of the whole genome as shown in Figure 1. *bZIP* genes distribution on chromosomes varies greatly and is uneven. For example, chromosomes 5 and 7 have the most TabZIP (24% and 13% respectively) but these TFs are less on chromosome 6 with 10 % distribution (Figure 1 (b)). Chromosome 2 and 3 contained twenty-six members (12% and 14%). Further, chromosomes 1 and 4 have 11 TabZIPs, with a 11% share in the genome. Interestingly, most of the genes are present near the ends of the chromosomes suggesting a dynamic gene expression trend opted by the *TabZIP* genes.

3.2 Genome-wide annotation of dimerization properties of bZIP transcription factors in bread wheat

A structure-based search of the wheat transcription factors databases such as ***expVIP*** and ***EnsemblPlants*** has identified 265 bZIP TFs in hexaploid wheat. To predict bZIP dimerization specificity in wheat, structural rules established for the human (Vinson *et al.* 2002), drosophila (Fassler *et al.* 2002), and *Arabidopsis* (Deppmann *et al.* 2004) were considered and are as follow-

(i) length of the leucine zipper,
(ii) placement of asparagine or a charged amino acid in the hydrophobic interface, and
(iii) presence of interhelical electrostatic interactions.

Though literature is scarce but predicted dimer partner choice is not random in these bZIPs, instead dimerization specificity is defined by 'g' and 'e' positions followed by the presence/absence of asparagine at the 'a' position in a heptad. Following the above-entrenched criteria, we have divided the bread wheat bZIPs into eleven groups. Supplementary figure 1 shows the amino acid alignment of 265 wheat bZIPs. The specifics presented below is in accordance with the observations. Figure 2 shows the color-coded interactions between the candidate TabZIPs used in the study. We have colored-coded the interactions based on the type of amino acids in the 'a', 'd', 'e', and 'g' positions in a heptad. Four colors have been used for g↔e′ interacting pairs. Green is for the attractive basic-acidic pairs (R (arginine) ↔ E (Glutamic acid) and K (Lysine) ↔ E), orange is for the attractive acidic-basic pairs (E↔R, E↔K, D (Aspartic acid) ↔R, and D↔K), red is for repulsive acidic pairs (E↔E and E↔D). Blue is for repulsive basic pairs (K↔K and R↔K), etc. We have colored the residue red for acidic and blue for basic if just one of the two amino acids in the g↔e ′ pair is charged. It is black if the 'a' or 'd' position is polar and purple if either is charged. The following features of the specific amino acid residues in the heptads, have been postulated below:

3.2.1 Eleven bZIP sub-groups in *T. aestivum*

Like other polyploid crops, sugarcane and cotton, Triticum aestivum, is a hexaploid crop. It contains 42 chromosomes with contributions from three, i.e., A, B, and D genomes and six allele copies in total. It gives three homoelog triad copies of every bZIP in hexaploidy wheat T aestivum. Here, group 1, the largest sub-family, is classified based on the presence of an N at the 'a' position in the 2nd heptad, comprising 86 members. Attractive acidic-basic and attractive basic-acidic g↔e′ interactions in the 1st, 2nd, 5th and 6th heptads. Additionally, repulsive g↔e′ interactions are present in 1st, 3rd, and 5th heptads favoring both the aspects of homo- and hetero-dimerization between the same TabZIP protein or within the sub-family. Furthermore, single repulsive acidic and basic amino acids are present at the 'g' and 'e' positions, individually deciphering the heterodimerization outcomes from this family member protein. The 1st heptad contains attractive g↔e′ acidic-basic interactions in this group. The presence of positively and negatively charged residues at the 'g' and 'e' positions instigates the electrostatic interactions. Its zipper (dimerization) region ends after the 6th heptad because of the presence of P, a helix breaker.

Group 2 is classified based on the presence of N at a position of 4th heptad. It also has glutamic acid at 'e' position in 2nd heptad of this group member. It is composed of a single bZIP protein which is nine heptads long.

Group 3 consists of 15 bZIPs. It is characterized by N at 'a' position in the 2nd and 4th heptad and attractive basic-acidic pairs (R↔E and K↔E) in heptads 1 and 2. Single repulsive acidic and basic amino acid residues in 1st, 2nd, and 3rd heptads are also present. This group contains heptad lengths ranging from 11 to 14. Concurrently, S is present at the '*a*' position in some of the members of this

group in the 1st heptad. The unique placement of N in the '*a'* position of the 2nd and 4th heptads will favor homo-dimerization.

In Group 4, there are 16 members. The attractive *g*↔*e′* pair in the 3rd heptad (except one) should favour homodimerization. There are repulsive interactions in 7th heptads (except three members) that may promote heterodimerization. The presence of N in '*a'* position of the 5th heptad should favour homodimerization within the group members. Incomplete and/or repulsive basic pairs in the 1st and 3rd heptads indicate likely heterodimerization with acid zipper proteins. The presence of attractive acidic-basic *g*↔*e′* interaction in 5th, 6th, and 9th heptads and attractive basic-acidic interaction in 7th heptad should lead to homodimerization., but will not impact much because of repulsive *g*↔*e′* acidic and basic amino acid abundance in initial heptads. These initial heptads are decisive for dimerization.

Group 5 comprises of 21 bZIP members. Placement of N in '*a'* position of 2nd and 5th heptad and an attractive *g*↔*e′* interaction in the 2nd heptad indicates homodimerization. The presence of repulsive *g*↔*e′* acidic and basic amino acid abundance in 2, 3, 4, 5 and 6 heptads, makes it the most complex group in defining dimerization fate.

Group 6 with 6 bZIP members having N at 'a' position in 2nd and 4th heptads. It has attractive basic-acidic *g*↔*e′* pairs in 1 and 2nd heptads and attractive basic-acidic *g*↔*e′* pairs in 4th heptads, suggesting homodimerization.

Group 7 has 20 bZIP members. The placement of N in the '*a'* position of the 5th heptad indicates homodimerization, but there is a likelihood of heterodimerization because of the presence of repulsive acidic and basic *g*↔*e′* pairs in 2, 3, and 7th heptads.

Group 8 has 56 bZIP members. It is expected to homodimerize due to the presence of N in the '*a'* position of the 1st and 5th heptads and two attractive *g*↔*e′* pairs in the 2nd, 3rd,5th, 6th, and 7th heptads. Similarly, the presence of repulsive acidic and basic *g*↔*e′* interactions in almost1,2,3,4,5,6 and 7 heptads of around 17 group members may lead to heterodimer formation with other groups.

Group 9 has 33 bZIP members. Attractive *g*↔*e′* interactions in the 5th, 6th, and 9th heptads and the presence of N in the '*a'* position of the 5th and 8th heptad suggests homodimerization. The presence of charged amino acids in '*g',* and *'e'* position in the 1st, 2nd, 4th, and 7th heptads followed by attractive *g*↔*e′* pairs in the 4th and 5th heptads may lead to the heterodimerization with other groups.

Like group 2, the group 10 is the smallest groups with one member strength with an unpredictable dimerization behaviour.

Finally group 11 has six bZIP members. It has a mix of attractive and repulsive *g*↔*e′* pairs but has N at '*a'* position in the 2nd, 5th and 9th heptads, encouraging homodimerization.

3.3 Features of a, d, g, and e positions amino acids in the leucine zipper domain of wheat bZIPs

The interaction interface reveals four critical sites in bZIP heptads, which play a pivotal role during the dimerization event. We have compared the features of these positions in *T. aestivum* with the data available from other reference species such as *Z mays*, *O sativa*, *H vulgare*, and *A thaliana* in Figure 3 (Deppmann *et al.* 2004; Nijhawan *et al.* 2008; Wei *et al.* 2012; Zhong *et al.* 2021) . Amino acids in the 'a' and 'd' positions of the leucine zipper are typically hydrophobic, with various amino acids in the 'a' position and predominately leucine in the 'd' position. An exception is a 2nd heptad 'a' position, which contains N in most homodimerizing bZIP proteins.

It is found that 21% of *T aestivum* bZIPs contain N at 'a' position suggesting homodimerization as N prefers to interact with N in the second monomer participating in the homodimerization. In addition, *T aestivum* has the highest concentration of hydrophobic amino acids among all plant species, with 37% of the 'a' position occupied by I, V, L, and M. It may prevent the higher order oligomerization, emphasizing the importance of 'a' positions equivalent to 'g' and 'e' positions in deciding the interaction fate. On the other hand, N at the 'a' position is highest in *Z mays* and suggests its inclination in forming homodimers. L at the 'd' position stabilizes the coiled-coil of bZIPs more effectively than any other amino acid in the hydrophobic interface. In a few cases, it is replaced by other hydrophobic aliphatic and aromatic amino acids, such as I, V, M, and F. In *T aestivum*, 46% of 'd' position has leucine, which is less than *A thaliana* (53%), *O sativa* (53%), *H vulgare* (49%), and *Z mays* (54%), suggesting that the gene families have undergone evolutionary modifications throughout the hybridization process. The 22 % occurrence of other amino acids at the 'd' position, such as I, V, and M, is highest in *T aestivum*.

All TabZIPs contain charged and long side-chain amino acids such as D, E, R, K, and Q in heptads. The presence of charged amino acids at the 'e' and 'g' positions is crucial. They augment (+ ↔ - or - ↔ + electrostatic interactions) or diminish (- ↔ - or + ↔ + interactions) the dimer formation among bZIPs depending on the types of amino acids present at these positions. In wheat, acidic amino acids D/E, with 31 %, are more common in the 'g' position than in Arabidopsis (27%) and less common than in *Z mays* (36%). On the contrary, the basic amino acids such as K/R are present in 24% of cases, the highest among all plant species except Z *mays* (29%). Besides, an abundance of D/E residues at the 'e' position is scant in *T aestivum* (12%), and is less than *Z mays* (23%), *O sativa* (13%), *A thaliana* (20%), and *H vulgare* (14%). Furthermore, *T aestivum* has a 25% distribution of K/R residues, higher than *O sativa* (22%) and *A thaliana* (22%).

3.4 Prediction of dimerization properties of candidate TabZIPs in wheat compared to the reference plant species

We have predicted the dimerization properties in the reference plant species (Oryza sativa, Zea mays, Hordeum vulgare, and Arabidopsis thaliana) used for the study with the entrenched structural rules of dimerization discussed in the previous section 3.1.1. Candidate TabZIPs and some putative bZIPs with a strong expression in different seed development stages, we have prepared the Supplementary figure 2 for *A thaliana, O sativa, Z mays,* and *H vulgare*. Furthermore, the dimerization properties of each species were compared with *T aestivum* data (Supplementary figure 2 (A)) to understand the differences between the plants used in the study and the significance of using *T aestivum* as a candidate plant species.

The dimerization specificity in the bZIPs is governed by a conserved structural rules (Vinson *et al.* 2002). Therefore, we have conceived the idea of classifying the candidate TabZIPs based on the amino acid present in each heptad. The amino acid sequence of these bZIPs in bread wheat is shown in the color-coded Supplementary figure 2 (A), aligned to show the dimerization potential. The N-terminal boundary is similar for all bZIP proteins defined by the presence of the clusters of basic amino acids. Further, conserved N residue in the basic region of all the bZIPs was used to align the bZIP sequences. We employed the same structural criteria used earlier for the dimerization prediction of the entire group in Supplementary figure 1.

The wheat bZIPs' leucine zipper region contains electrostatic interactions that are both attractive and repulsive. These interactions are shown in colored boxes and are used to predict the dimerization potential of a specific bZIP protein. Observations are consistent with the bZIP families identified in Humans, Drosophila, Arabidopsis, and cereal crops like rice and maize (Fassler *et al.* 2002; Jakoby *et al.* 2002; Vinson *et al.* 2002; Nijhawan *et al.* 2008; Wei *et al.* 2012). The distinct combination of amino acids at the a, d, e, and g positions creates a new set of structural guidelines for determining the species-specificity of leucine zipper dimerization (Deppmann *et al.* 2004)

bZIP proteins regulate the function of target genes by forming homo- or heterodimers. To determine the molecular basis of heterodimer formation between TabZIP proteins, we analyzed their propensities to form dimeric complexes.

3.4.1 Homo- and Heterodimerization potential within the candidate TabZIPs

The key step for each bZIP in every species is determining the likelihood of selecting the suitable dimerization partners, which ensures the success of the dimerization process. Figure 2 illustrates the homo- and heterodimerization properties of the candidate TabZIPs analyzed in this study, highlighting the possible interaction patterns among them.

TraesCS5B02G470600 (EmBP1) TF has three attractive acidic-basic pairs and four repulsive acidic or basic pairs. Out of the repulsive pairs, three incomplete and one complete acidic pair are present. Again, in the second heptad of next pair TraesCS5B02G470600 (EmBP1) with TraesCS7D02G518100,

TraesCS1A02G072600, and TraesCS3D02G364900 (ABI5), there is anticipatory formation of heterodimers between repulsive basic amino acid residues K↔K', K↔Q', and K↔K' at g↔e' positions. Following the dimerization trend between the TraesCS5B02G470600 and TraesCS7D02G518100 having K↔K' at g↔e' positions in the fourth heptad of their sequences.

Secondly, TraesCS7A02G398400 being the weakest TabZIP possesses incomplete dimerization potential due to lack of charged amino acid residues at the 'g' and e positions. There is little possibility of even homodimerization taking place and no possibility of its participation in heterodimerization.

Thirdly, TraesCS3D02G364900 (ABI5) has two attractive acidic-basic electrostatic interactions and four repulsive acidic and basic pairs. This is an indication of heterodimerization of this protein. TraesCS3D02G364900 (ABI5) after one repulsive electrostatic interaction in the second heptad with TraesCS5B02G470600 (EmBP1) is enthralling the repulsive Q↔E' interaction at *e↔g'* positions in the sixth heptad iteratively.

Further, TraesCS7D02G518100 contains an equal number of attractive and repulsive pairs, so it is predicted to form both homo- and heterodimers. We have observed that due to the presence of E↔Q' at g↔e' positions in the second heptad position in TraesCS7D02G518100 and TraesCS1A02G072600 pair, there is a possibility of heterodimerization in the sequence. A similar observation in the second heptad is made between TraesCS7D02G518100 and TraesCS7A02G398400, where repulsive E↔E' pair has been seen at g↔e' positions with the possibility of strong heterodimerization initiation at second heptad.

TraesCS5D02G124600 (TabZIP1), which has two favorably interacting pairs and five repulsive pairs, is more likely to heterodimerize. Additionally, TraesCS1A02G072600, the most conspicuous member with four repulsive pairs and one attractive pair, is the primary TabZIP with heterodimerization propensity. In the next pair between TraesCS1A02G072600 and TraesCS7A02G398400, repulsive acidic residues are present at g↔e', indicative of heterodimerization. Furthermore, TraesCS1A02G072600, has repulsive acidic pairs E↔E' and D↔E' at g↔e' positions with TraesCS5B02G470600.

3.5 Experimental validation of dimerization properties of bZIP transcription factors in bread wheat

A) bZIP TFs protein expression within prokaryotic expression system

Wheat bZIP transcription factors have not been sufficiently characterized at the molecular level due to a lack of cloning and recombinant protein production of wheat bZIPs. Therefore, we started with cloning, and the expression of recombinant wheat bZIP proteins in bacterial system. DNA binding region and leucine Zipper region of bZIPs were amplified as BamHI and HindIII fragments from cDNA

templates prepared from respective developmental stages. For the experimental validation of dimerization potential analysis of wheat bZIPs, we cloned seed-specific bZIP TFs in pET23+ vector and expressed in E. coli (BL21 DE3) expression system. All bZIPs have a T7 tag and protein lysate was dialyzed against the low salt buffer. Further, protein lysate was applied to the Heparine-sepharose column and protein was eluted using 1M KCl elution buffer (1M KCl, KPO_4 buffer, pH 7.4) as shown in Figure 4. Details for further downstream processing and purification steps are provided in the supplementary file S1.

3.5.1 Secondary structure prediction and Thermal stability analysis of TabZIP proteins

To evaluate the thermal stability of all eight candidate TaZIP proteins used in this study, we used circular dichroism spectroscopy at 222 nm to monitor their thermal stability. Figure 5 shows the wavelength scan and temperature-induced melting curves of TraesCS1A02G072600, TraesCS7D02G518100, TraesCS5B02G470600 (EmBP1), TraesCS3D02G364900 (ABI5), TraesCS7A02G398400, TraesCS5D02G124600 (TabZIP1) with 2 µM protein concentration. CD data of TraesCS5A02G237200 (and its mutant TraesCS5A02G23560) and TraesCS4B02G320400 has been shown in Figures 7 and 8 respectively. All proteins showed the cooperative unfolding as the temperature was increased from 6-85° C. Each melting curve was fitted to an equation (equation 1) that describes the equilibrium constant (Kd) as a function of temperature. Assuming the thermal denaturation of leucine zipper domains to be of a two-state type, each melting curve was fitted that gave values of T_m and ΔH_m. Slope of a linear fit of Tm Vs ΔH_m gave the value of ΔC_p in kcal mol-1K-1(Table 1). This along with Tm and ΔHm values were used to obtain ΔG_D at 25˚ C in Figure 5 A-C panels. All such thermodynamic stability parameters are given in Table 1. Proteins with cysteine residues in the sequence were pre-heated for fifteen minutes with DTT before melting. TraesCS7D02G518100, the most stable transcription factor employed in the study, with the greatest Tm (64°C) and ΔG_D value, exhibits exceptional behaviour. Rest of the candidates, such as TraesCS1A02G072600, TraesCS5B02G470600 (EmBP1), TraesCS3D02G364900 (ABI5), TraesCS7A02G398400, TraesCS5D02G124600 (TabZIP1) follow the typical bZIP transcription factor behaviour with Tm range between 36-47°C. Rest two TabZIPs, TraesCS5A02G237200 (and its mutant TraesCS5A02G23560) and TraesCS4B02G320400 considered for the amino acid variations and leucine zipper length features respectively, exhibited Tm ranging from 38˚C to a stable Tm 52˚C. All thermal denaturation results were observed to be reversible, with Subtle changes in Tm values more/less than 2˚C in case of all proteins used in the study except TraesCS5A02G237200 with more changes after heat exposure till 85˚C temperature being a homeolog with an unstable thermal behaviour of 30˚C.

3.5.2 Protein- protein interaction analysis of TabZIPs

We employed MALDI-TOF to investigate the protein-protein interaction fate or dimer forming capability between the six candidate TabZIPs. It is assumed that a heterodimer between two proteins will be formed only if it is more stable than either of the homodimers in a mixture.

TraesCS7D02G518100 is more stable and shows higher Tm (63˚C) and ΔG_D values compared to other TabZIPs used in this study. MALDI-TOF MS traces are shown in Figure 6 and the mass of TabZIPs have been provided in Table 1. TraesCS3D02G364900 (ABI5), a well-studied bZIP shows the monomeric monoisotopic peak, and a dimer peak is also observed. TraesCS3D02G364900 (ABI5) contains charged amino acid residues at 'g' and 'e' positions in the first six heptads. It also may heterodimerize with other bZIP such as TraesCS1A02G072600, TraesCS7A02G398400, and TraesCS5B02G470600 (EmBP1).

Here we show that TraesCS1A02G072600 may heterodimerize with TraesCS5B02G470600 (EmBP1). Supplementary figure 3 shows the MALDI-TOF graph of each mono- and dimeric ion peak for all six TabZIPs considered for the in-vitro protein-protein interaction study. Similarly, TraesCS7A02G398400 dimerizes with TraesCS5B02G470600 (EmBP1). The two TabZIPs such as TraesCS5B02G470600 (EmBP1) and TraesCS3D02G364900 (ABI5), demonstrate dimerization potential not seen in other bZIPs studied here.

3.6 Identifying the amino acid substitution and heptad length impact on the dimerization properties in TabZIPs

We tried to extend and validate the earlier gene expression data by structural analysis approach to study the amino acid sequences in TraesCS5A02G237200 (Kaur *et al.* 2024). Different amino acids present in TraesCS5A02G237200 owe additional electrostatic interaction fate to its homeolog (TraesCS5A02G235600) present on the B-subgenome (Figure 7). The higher coupling energy dimension from the literature goes in synergy with our results when we see the occurrence of glutamine (Q) and alanine (A) in TraesCS5A02G237200 with Tm 30˚C compared to a significant shift to 43˚C in mutant homeologs TraesCS5A02G235600 and TraesCS5A02G244500 having glutamic acid (E) and lysine (K) instead of Q and A in their sequence.

The alignment of 265 protein sequences (Supplementary figure 1) revealed remarkable observations regarding the length of bZIP proteins in wheat compared to human and mouse. Notably, wheat bZIPs tend to be longer, with some extending up to 14 heptads, such as TraesCS4B02G320400. To assess the stability of these extended coiled-coil structures, truncated variants of TraesCS4B02G320400 were designed, ranging from the minimum required 4 heptads (for the helical dimerization between two monomers) to the full 14-heptad length. Thermal denaturation experiments revealed distinct T_m values for each variant. The shortest variant (4 heptads) exhibited a T_m of 37°C, while longer variants displayed varying levels of stability: 6 heptads (50°C), 8 heptads (44°C), 10 heptads (53°C), 12 heptads (50°C), and 14 heptads (45°C) as shown in Figure 8. The variation in T_m across different lengths suggests that

459 the addition of amino acids such as glutamic acid (E), lysine (K), aspartic acid (D), arginine (R) etc. at
460 'g' and 'e' positions, influence structural stability, likely due to differences in residue composition and
461 electrostatic interactions. Analysis of the heptad positions in TraesCS4B02G320400 revealed the
462 presence of serine (S), alanine (A), valine (V), isoleucine (I), and cysteine (C) at the 'a' position,
463 suggesting a higher potential for heterodimer formation. Notably, a single asparagine (N) was observed
464 in the fifth heptad, which may further indicate homo- dimerization specificity. The diversity of residues
465 at the 'a' position indicates possible variations in coiled-coil interactions, contributing to the structural
466 adaptability of the bZIP protein.

467 **Discussion**

468 Wheat is a low-cost cereal crop. Its grains are a major source of human calories, and wheat straw is
469 used as an animal feed (Awika 2011). Since the draft genome is of Chinese spring cv. *T aestivum*, we
470 proceeded to use the data of this variety. 265 projected bread wheat bZIPs can produce 35, 245 dimers,
471 demonstrating the enormous potential of gene regulation. The DNA binding class of transcription
472 factors follow the dynamic gene expression by occurring at distal ends of chromosomes (Mak *et al.*
473 2009). In our analysis, a smaller percentage of bZIP transcription factors were detected in the
474 centromeric regions of the chromosomes, whereas the majority were found in the distal ends. This non-
475 random distribution points to a possible cause of expression asymmetry, which is probably impacted by
476 the number of regulatory elements and chromatin accessibility (Smith *et al.* 2011; Perea-Resa and
477 Blower 2018). Furthermore, this pattern might be a reflection of traits linked to the polyploid
478 background, where the genomic organisation of transcription factors is influenced by processes for gene
479 retention and dosage balancing (Conant *et al.* 2014; Cheng *et al.* 2018).

480 In nature, dimerization is one way the transcription factors increase their repertoire of
481 recognized DNA sequences. Heterodimerization results in the reorganization of novel DNA sequences
482 leading to new functions (Deppmann *et al.* 2004; Rodríguez-Martínez *et al.* 2017). All bZIPs proteins
483 are aligned with the invariable N in the DNA-binding domain of the proteins. Further, the presence
484 of R/K at the eighth position c-terminal to invariable N and L at the thirteenth position, followed by
485 L or any other hydrophobic amino acid at every seventh position or 'a' position of a heptad and the
486 presence of charged amino acid at 'e' and 'g' position regards a sequence as a bona fide bZIP TF. P
487 or two Gs, both natural helix-breakers, establish the bZIP coiled-coil limit at the c-terminal. Out of
488 294, 29 TabZIPs do not contain a defined bZIP domain and are misclassified under the bZIP family
489 as they contain the conserved bHLH- and DOF- domains in their sequence. We have excluded these
490 transcription factors in our analysis. The alignment of 265 protein sequences led to a few remarkable
491 observations. 1) Compared to human and mouse wheat bZIPs are long. In some cases, they are up
492 to 14 heptads long. Initially, we didn't anticipate the possibility of such a lengthy coiled-coil to be
493 stable, this hypothesis was also validated in this study. 2) Unlike mammals, wheat bZIPs have a high

494 propensity to form homodimers. 3) Numerous wheat bZIPs feature intricate combinations of amino
495 acids, making it challenging to predict dimerization fate. 4) bZIP homeologs in bread wheat show
496 amino acid substitutions, ranging from single to multiple residue variations due to polyploid nature
497 of evolution. Validation of these sequence differences led to the recognition of homeolog expression
498 switches under different stress and developmental conditions, highlighting the dynamic regulation
499 of homeolog-specific gene expression.

500 To extend our study on the functional side of TabZIPs, we have expanded the biophysical
501 analysis of these proteins to determine how the particular a, d, e, and g locations relate to dimerization
502 stability. In wheat, we observed that N at 'a' position is present in a low proportion (21%) compared to
503 other model plant species i.e., *A thaliana* and other plant species like *Z mays* (26%). We have observed
504 the presence of amino acids S, C, K, A, and Q at 'a' position, especially in the initial four heptads, which
505 is uncommon in reference plants such as *Z mays, O sativa, H vulgare and A thaliana*. The amino acids
506 such as S and A are abundant in TabZIPs in instead of N at 'a' position. Amino acid S can be
507 phosphorylated; such modification may change the fate of dimerization and DNA binding (Lee *et al.*
508 2010). Similarly, A is involved in the stress response such as heat and drought environments (Kusano
509 *et al.* 1995).

510 The α-helical structure is detected in the bZIP proteins by measuring the ellipticity by the CD
511 spectroscopy (Acharya *et al.* 2002). bZIP dimers unfold reversibly and cooperatively to produce
512 monomers in heat and chemical denaturants. The thermal denaturation curves of human bZIPs are well
513 represented by the two-state model allowing the study of individual amino acids contribution to the
514 dimerization specificity (Acharya *et al.* 2002, 2006). In bread wheat, we observed the two-state thermal
515 denaturation curve during the thermal stability analysis for all eight TabZIPs. In addition, we looked for
516 the reversibility trend in the TabZIPs to study the structural changes in the α-helical structure after the
517 temperature exposure from 6 upto 85˚C at the rate of 1° C/min by measuring the change in ellipticity at
518 222 nm wavelength. All eight bZIPs appeared to reverse with quite subtle changes in the ellipticity but
519 TraesCS5A02G237200.

520 To determine the molecular basis of heterodimer formation between TabZIP proteins, we
521 analyzed their propensities to form dimeric complexes. As described in section 3.1.1, we grouped the
522 bZIPs based on invariable 'N', 'R' in DNA binding domain and 'L' and charged amino acids in the leucine
523 zipper region (Acharya *et al.* 2002). In case of TraesCS5B02G470600 (EmBP1) with
524 TraesCS7D02G518100, TraesCS1A02G072600, and TraesCS3D02G364900 (ABI5) bZIPs, we predicted
525 that based on the presence of N at 'a' position in second heptad these proteins should form a homodimer,
526 but the repulsive basic amino acid residues K↔K', K↔Q', and K↔K' at g↔e' positions in second heptads
527 should encourage heterodimerization. MALDI-TOF studies further experimentally validated these
528 predictions (Figure 6 and Supplementary figure 3).

In Arabidopsis, during seed maturation, it has been shown that the bZIP53 forms a heterodimer complex with the bZIP10, and bZIP25 (Alonso *et al.* 2009; Jain *et al.* 2017). Being polyploid, bread wheat confers the homeolog copies of each gene expressing under the specific developmental and stress response due to genetic and epigenetic reasons. In our earlier research, the genetic basis of the differences in protein sequences of bZIP triads was explored, which may impart structural stability to a specific homeolog enabling the plant to endure the stress conditions better (Kaur *et al.* 2024). Previous research has examined how each amino acid contributes to the specificity of dimerization in humans (Vinson et al. 2002), drosophila (Fassler et al. 2002), and *Arabidopsis* (Deppmann et al. 2004). In addition to these studies, single α-helical domain enriched with amino acid residues such as E, R, K and H, stabilise the α-helices through salt bridges (Steinmetz *et al.* 2007). In line with these findings, we observed a similar trend in TraesCS5A02G237200, which exhibited an unstable thermal denaturation profile with a melting temperature (T_m) of 30°C. On the other hand, the mutant homeolog TraesCS5B02G235600 displayed a significantly higher T_m of 43°C, indicating increased structural stability. This difference can be attributed to the presence of glutamic acid (E) and lysine (K) replacing the glutamine (Q) and alanine (A) respectively, in the second and third heptad positions of TraesCS5B02G235600, which provide additional electrostatic interactions. These findings emphasize the critical role of charged residues in the dimerization and stable coiled-coil formation, reinforcing the importance of electrostatic interactions in protein stability and function.

Previous studies have identified a maximum of five heptads in human bZIP proteins, suggesting that beyond this length, additional heptads may not significantly enhance dimerization efficiency (Vinson *et al.* 2002). In contrast, our findings in wheat bZIPs reveal extended coiled-coil domains, reaching up to 14 heptads, which raises intriguing questions about the evolutionary and functional significance of these longer sequences. The presence of additional heptads in wheat bZIPs may contribute to increased stability, altered dimerization specificity, or distinct regulatory mechanisms compared to their human counterparts. (Vinson *et al.* 2002). For TraesCS4B02G320400, leucine zipper length was the key criterion to assess its impact on protein behaviour. We hypothesized that beyond 7 to 9 heptads, the helical structure would begin to destabilize. Contrary to our expectations, the variants ranging from 6 to 14 heptads exhibited remarkable stability, with melting temperatures (Tm) ranging from 50–52°C, exceptionally stable compared to the 4-heptad variant, which had a Tm of 38°C. Our findings highlight that the longer leucine zippers, uniquely found in bread wheat compared to other plant species, as well as human and mouse, likely contribute to protein stability. This enhanced stability may be linked to the polyploid nature of bread wheat, providing functional advantages in its regulatory networks (Evans *et al.* 2022).

Conclusion

In conclusion, creating new wheat varieties with enhanced agronomic features and comprehending the basic biology of polyploid organisms depend on the dimerization potential of each TabZIP protein and asymmetric gene expression in wheat. Contribution of amino acids at specific heptad positions in TabZIPs and the sequence based structural variations in the bZIP homeologs owe specific biochemical features and helps to withstand the stress response by additional electrostatic interaction possibilities within the forming bZIP dimers. Further investigations are necessary to determine whether the extended length of bZIP domains in bread wheat, provides functional advantages in plant-specific transcriptional regulation. Moreover, the insights gained during the study could aid in breeding strategies in crop improvement by manipulating individual or multiple homeologs to modulate trait response.

Acknowledgments

RK and VR thank the National Agri-Food Biotechnology Institute (NABI) Executive Director, Mohali, for research facilities and the Department of Biotechnology (DBT), New Delhi, for funding. RK acknowledges the Department of Science and Technology (DST) for the DST-Inspire fellowship.

Competing Interest

Authors declare no competing interest.

Conflict of Interest

The authors declare no conflict of interest regarding the research.

Author contribution

Raminder Kaur: Conceptualization, Writing – original draft, Visualization, Validation, Methodology, Investigation, Data curation, Formal analysis, Review & editing. **Nishtha Sharma:** Review & editing. **Prateek Jain:** Review & editing. **Mamta Verma:** Review & editing. **Ashish Apkari:** Review & editing. **Vikas Rishi:** Conceptualization, Methodology, Writing – original draft, Writing – review & editing, Methodology, Investigation, Formal analysis, Supervision, Review & editing, Project administration, Funding acquisition.

References

Acharya A, Rishi V, Vinson C (2006) 'Stability of 100 homo and heterotypic coiled-coil a-a′ pairs for ten amino acids (A, L, I, V, N, K, S, T, E, and R)' *Biochemistry* **45**, 11324–11332. doi:10.1021/bi060822u

Acharya A, Ruvinov SB, Gal J, Moll JR, Vinson C (2002) 'A heterodimerizing leucine zipper coiled coil system for examining the specificity of a position interactions: Amino acids I, V, L, N, A, and K' *Biochemistry* **41**, 14122–14131. doi:10.1021/bi020486r

Alonso R, Oñate-Sánehez L, Weltmeier F, Ehlert A, Diaz I, Dietrich K, Vicente-Carbajosa J, Dröge-Laser W (2009) 'A Pivotal Role of the Basic Leucine Zipper Transcription Factor bZIP53 in the Regulation of arabidopsis Seed Maturation Gene Expression Based on Heterodimerization and Protein Complex FormationW' *Plant Cell* **21**, 1747–1761. doi:10.1105/tpc.108.062968

Awika JM (2011) Major cereal grains production and use around the world. In 'ACS Symp. Ser.', doi:10.1021/bk-2011-1089.ch001

Baxevanis AD, Vinson CR (1993) 'Interactions of coiled coils in transcription factors: where is the specificity?' *Current Opinion in Genetics and Development* **3**, 278–285. doi:10.1016/0959-437X(93)90035-N

Cheng F, Wu J, Cai X, Liang J, Freeling M, Wang X (2018) 'Gene retention, fractionation and subgenome differences in polyploid plants' *Nat. Plants* **4**,. doi:10.1038/s41477-018-0136-7

Conant GC, Birchler JA, Pires JC (2014) 'Dosage, duplication, and diploidization: Clarifying the interplay of multiple models for duplicate gene evolution over time' *Curr. Opin. Plant Biol.* **19**,. doi:10.1016/j.pbi.2014.05.008

Deppmann CD, Acharya A, Rishi V, Wobbes B, Smeekens S, Taparowsky EJ, Vinson C (2004) 'Dimerization specificity of all 67 B-ZIP motifs in Arabidopsis thaliana: A comparison to Homo sapiens B-ZIP motifs' *Nucleic Acids Research* **32**, 3435–3445. doi:10.1093/nar/gkh653

Deppmann CD, Alvania RS, Taparowsky EJ (2006) 'Cross-species annotation of basic leucine zipper factor interactions: Insight into the evolution of closed interaction networks' *Mol. Biol. Evol.* **23**, 1480–1492. doi:10.1093/molbev/msl022

Dröge-Laser W, Snoek BL, Snel B, Weiste C (2018) 'The Arabidopsis bZIP transcription factor family — an update' *Curr. Opin. Plant Biol.* **45**, 36–49. doi:10.1016/j.pbi.2018.05.001

Ellenberger TE, Brandl CJ, Struhl K, Harrison SC (1992) 'The GCN4 basic region leucine zipper binds DNA as a dimer of uninterrupted α Helices: Crystal structure of the protein-DNA complex' *Cell* **71**, 1223–1237. doi:10.1016/S0092-8674(05)80070-4

Evans CEB, Arunkumar R, Borrill P (2022) 'Transcription factor retention through multiple polyploidization steps in wheat' *G3: Genes, Genomes, Genetics* **12**,. doi:10.1093/g3journal/jkac147

Fassler J, Landsman D, Acharya A, Moll JR, Bonovich M, Vinson C (2002) 'B-ZIP proteins encoded by the Drosophila genome: Evaluation of potential dimerization partners' *Genome Research* **12**, 1190–1200. doi:10.1101/gr.67902

625 Foster R, Izawa T, Chua N (1994) 'Plant bZIP proteins gather at ACGT elements' *The FASEB*
626 *Journal* **8**,. doi:10.1096/fasebj.8.2.8119490

627 Jain P, Shah K, Sharma N, Kaur R, Singh J, Vinson C, Rishi V (2017) 'A-ZIP53, a dominant negative
628 reveals the molecular mechanism of heterodimerization between bZIP53, bZIP10 and bZIP25
629 involved in Arabidopsis seed maturation' *Scientific Reports* **7**,. doi:10.1038/s41598-017-14167-
630 5

631 Jakoby M, Weisshaar B, Dröge-Laser W, Vicente-Carbajosa J, Tiedemann J, Kroj T, Parcy F (2002)
632 'bZIP transcription factors in Arabidopsis' *Trends in Plant Science* **7**, 106–111.
633 doi:10.1016/S1360-1385(01)02223-3

634 Kaur R, Singh D, Singh PK, Kaur G, Shah K, Pandey H, Devi SG, Pandey AK, Rishi V (2024)
635 'Identifying the genetic and epigenetic basis for asymmetric bZIP expression in temperature-
636 stressed bread wheat' *Plant Growth Regulation* **103**,. doi:10.1007/s10725-024-01129-x

637 Kelly SM, Jess TJ, Price NC (2005) 'How to study proteins by circular dichroism' *Biochim. Biophys.*
638 *Acta - Proteins Proteomics* **1751**,. doi:10.1016/j.bbapap.2005.06.005

639 Krylov D, Barchi J, Vinson C (1998) 'Inter-helical interactions in the leucine zipper coiled coil dimer:
640 pH and salt dependence of coupling energy between charged amino acids' *Journal of Molecular*
641 *Biology* **279**, 959–972. doi:10.1006/jmbi.1998.1762

642 Krylov D, Mikhailenko I, Vinson C (1994) 'A thermodynamic scale for leucine zipper stability and
643 dimerization specificity: e and g interhelical interactions' *EMBO Journal* **13**, 2849–2861.
644 doi:10.1002/j.1460-2075.1994.tb06579.x

645 Kusano T, Berberich T, Harada M, Suzuki N, Sugawara K (1995) 'A maize DNA-binding factor with
646 a bZIP motif is induced by low temperature' *MGG Molecular & General Genetics* **248**, 507–
647 517. doi:10.1007/BF02423445

648 Landschulz WH, Johnson PF, McKnight SL (1988) 'The leucine zipper: A hypothetical structure
649 common to a new class of DNA binding proteins' *Science* **240**, 1759–1764.
650 doi:10.1126/science.3289117

651 Lee S, Shuman JD, Guszczynski T, Sakchaisri K, Sebastian T, Copeland TD, Miller M, Cohen MS,
652 Taunton J, Smart RC, Xiao Z, Yu L-R, Veenstra TD, Johnson PF (2010) 'RSK-Mediated
653 Phosphorylation in the C/EBPβ Leucine Zipper Regulates DNA Binding, Dimerization, and
654 Growth Arrest Activity' *Molecular and Cellular Biology* **30**,. doi:10.1128/mcb.00782-09

655 Mak HC, Pillus L, Ideker T (2009) 'Dynamic reprogramming of transcription factors to and from the

656 subtelomere' *Genome Research* **19**,. doi:10.1101/gr.084178.108

657 Moitra J, Szilák L, Krylov D, Vinson C (1997) 'Leucine is the most stabilizing aliphatic amino acid in
658 the d position of a dimeric leucine zipper coiled coil' *Biochemistry* **36**, 12567–12573.
659 doi:10.1021/bi971424h

660 Newman JRS, Keating AE (2003) 'Comprehensive identification of human bZIP interactions with
661 coiled-coil arrays' *Science* **300**, 2097–2101. doi:10.1126/science.1084648

662 Nijhawan A, Jain M, Tyagi AK, Khurana JP (2008) 'Genomic survey and gene expression analysis of
663 the basic leucine zipper transcription factor family in rice' *Plant Physiology* **146**, 333–350.
664 doi:10.1104/pp.107.112821

665 Pathak D, Sigler PB (1992) 'Updating structure-function relationships in the bZip family of
666 transcription factors' *Curr. Opin. Struct. Biol.* **2**, 448. doi:10.1016/0959-440X(92)90238-3

667 Perea-Resa C, Blower MD (2018) 'Centromere Biology: Transcription Goes on Stage' *Molecular and*
668 *Cellular Biology* **38**,. doi:10.1128/mcb.00263-18

669 Riechmann JL, Ratcliffe OJ (2000) 'A genomic perspective on plant transcription factors' *Curr. Opin.*
670 *Plant Biol.* **3**,. doi:10.1016/S1369-5266(00)00107-2

671 Rodríguez-Martínez JA, Reinke AW, Bhimsaria D, Keating AE, Ansari AZ (2017) 'Combinatorial
672 bZIP dimers display complex DNA-binding specificity landscapes' *eLife* **6**,.
673 doi:10.7554/eLife.19272

674 Smith JJ, Miller LR, Kreisberg R, Vazquez L, Wan Y, Aitchison JD (2011) 'Environment-responsive
675 transcription factors bind subtelomeric elements and regulate gene silencing' *Molecular Systems*
676 *Biology* **7**,. doi:10.1038/msb.2010.110

677 Steinmetz MO, Jelesarov I, Matousek WM, Honnappa S, Jahnke W, Missimer JH, Frank S,
678 Alexandrescu AT, Kammerer RA (2007) 'Molecular basis of coiled-coil formation' *Proceedings*
679 *of the National Academy of Sciences of the United States of America* **104**, 7062–7067.
680 doi:10.1073/pnas.0700321104

681 Vinson C, Acharya A, Taparowsky EJ (2006) 'Deciphering B-ZIP transcription factor interactions in
682 vitro and in vivo' *Biochim. Biophys. Acta - Gene Struct. Expr.* **1759**, 4–12.
683 doi:10.1016/j.bbaexp.2005.12.005

684 Vinson C, Myakishev M, Acharya A, Mir AA, Moll JR, Bonovich M (2002) 'Classification of Human
685 B-ZIP Proteins Based on Dimerization Properties' *Molecular and Cellular Biology* **22**, 6321–
686 6335. doi:10.1128/mcb.22.18.6321-6335.2002

687 Vinson CR, Sigler PB, McKnight SL (1989) 'Scissors-grip model for DNA recognition by a family of
688 leucine zipper proteins' *Science* **246**, 911–916. doi:10.1126/science.2683088

689 Wei K, Chen J, Wang Y, Chen Y, Chen S, Lin Y, Pan S, Zhong X, Xie D (2012) 'Genome-wide
690 analysis of bZIP-encoding genes in maize' *DNA Research* **19**, 463–476.
691 doi:10.1093/dnares/dss026

692 ZADOKS JC, CHANG TT, KONZAK CF (1974) 'A decimal code for the growth stages of cereals'
693 *Weed Research* **14**,. doi:10.1111/j.1365-3180.1974.tb01084.x

694 Zhang L, Liting Wang JX, Si L, Zheng S, Yang Y, Yang H, Tian S (2020) 'Wheat TabZIP8, 9, 13
695 participate in ABA biosynthesis in NaCl-stressed roots regulated by TaCDPK9-1' *Plant*
696 *Physiology and Biochemistry* **151**,. doi:10.1016/j.plaphy.2020.03.039

697 Zhong X, Feng X, Li Y, Guzmán C, Lin N, Xu Q, Zhang Y, Tang H, Qi P, Deng M, Ma J, Wang J,
698 Chen G, Lan X, Wei Y, Zheng Y, Jiang Q (2021) 'Genome-wide identification of bzip
699 transcription factor genes related to starch synthesis in barley (Hordeum vulgare l.)' *Genome*
700 **64**,. doi:10.1139/gen-2020-0195

701

702 **Figures**

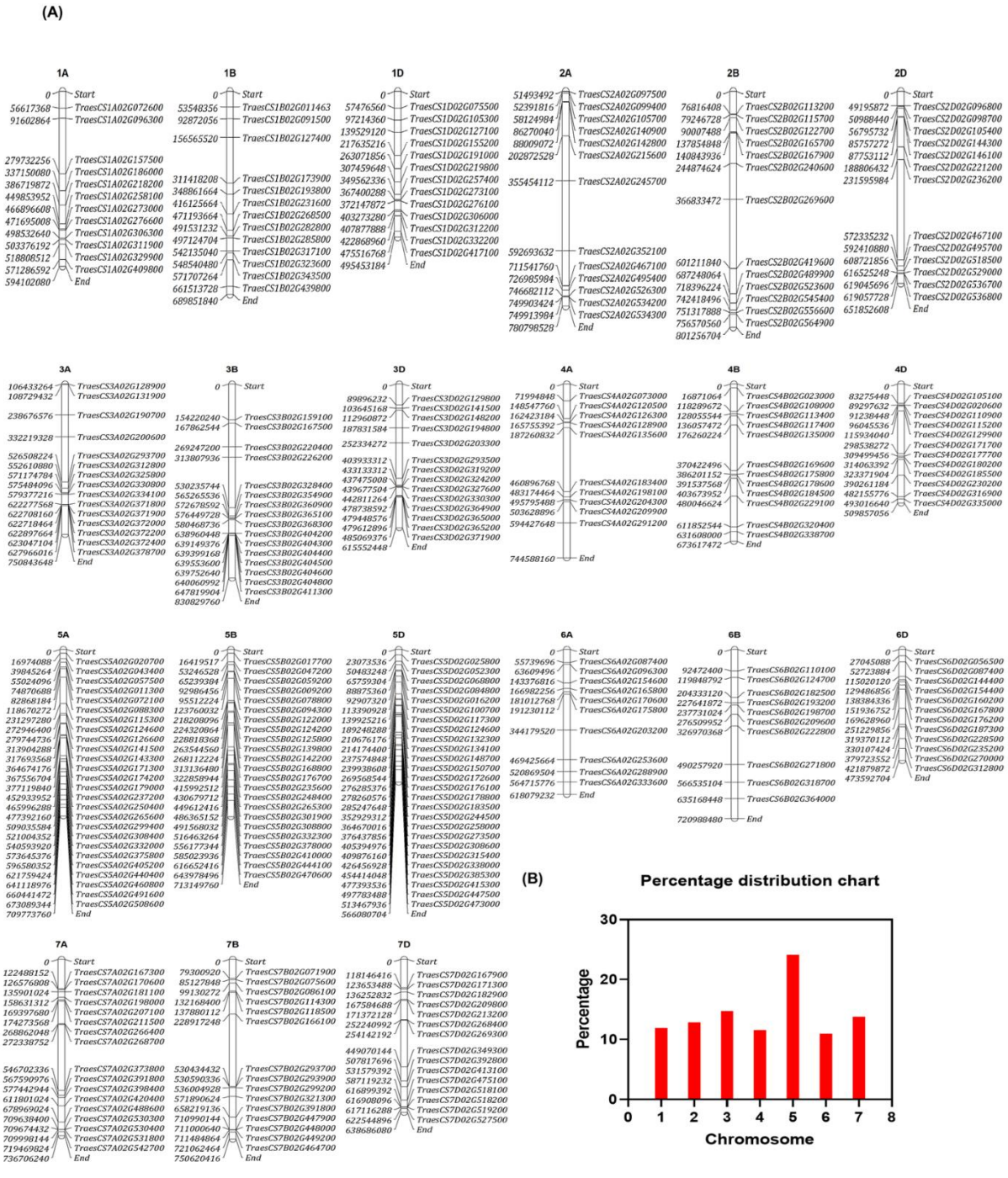

Figure 1 Genome wide distribution of TabZIPs on wheat chromosomes. (A) Distribution of bZIP proteins is represented on wheat genome on the basis of their chromosomal locations. Each chromosome is represented with black color (B) panel shows the percentage distribution of bZIPs on all chromosomes.

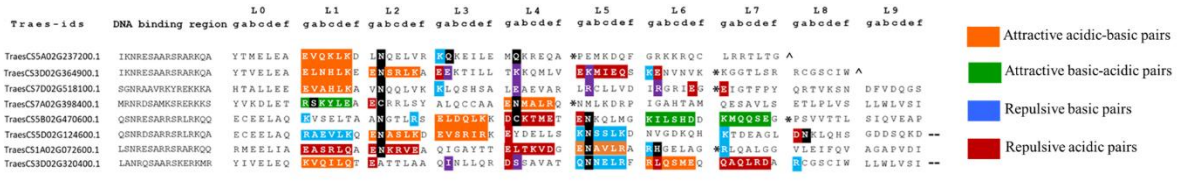

Figure 2 Amino acid sequence of all identified TabZIPs in bread wheat. Protein sequences are aligned based on the similarity in sequence. Second column contains Traes ids. Third column has n-terminal region of bZIP domain and c-terminal leucine zipper region is divided into heptads (a,b,c,d,e,f and g). Primarily, the placement of N at 'a' position was considered for classification and it was coloured black at the respective 'a' position. Secondarily, for the g-e' interactions, we used four colours (provided on the below right side). The attractive acidic-basic pairs (E↔R', E↔K', D↔R', D ↔K') were coloured orange, and the attractive basic-acidic pairs (R↔E, K↔E') were coloured green. We coloured the repulsive basic pairs (K↔K', R↔K') with blue and repulsive acidic pairs (E↔E', D↔D', E↔D') with red. We have coloured the polar residues black at 'a' and 'd' position and charged residues at 'a' and 'd' positions were coloured purple. The candidate genes have been divided into five groups. We have used (*)symbol for potential helix break, due to the presence of proline or glycine. Symbol (^) denotes the natural end of a bZIP protein, and (--) shows that it is a longer protein and we have only shown the 9 heptads in the coloured figure.

(A)

'a' position
'd' position
'g' position
'e' position
T aestivum
Z mays
O sativa
H vulgare
A thaliana
IVLM N Others
L IVM Others
DE KR Others
DE KR Others

(B)

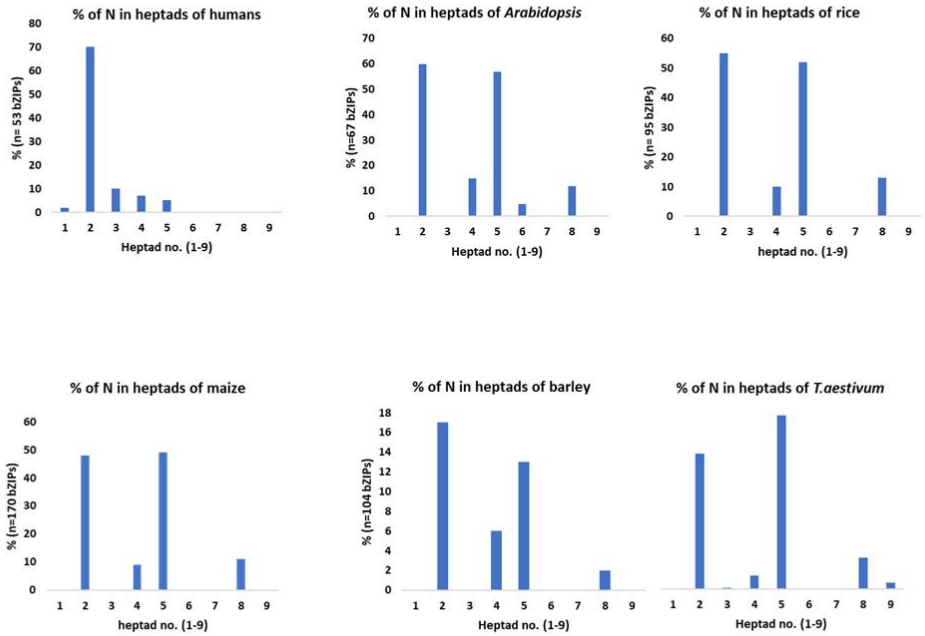
% of N in heptads of humans
% (n= 53 bZIPs)
Heptad no. (1-9)
% of N in heptads of Arabidopsis
% (n=67 bZIPs)
Heptad no. (1-9)
% of N in heptads of rice
% (n= 95 bZIPs)
heptad no. (1-9)
% of N in heptads of maize
% (n=170 bZIPs)
heptad no. (1-9)
% of N in heptads of barley
% (n=104 bZIPs)
Heptad no. (1-9)
% of N in heptads of T.aestivum
Heptad no. (1-9)

(C)

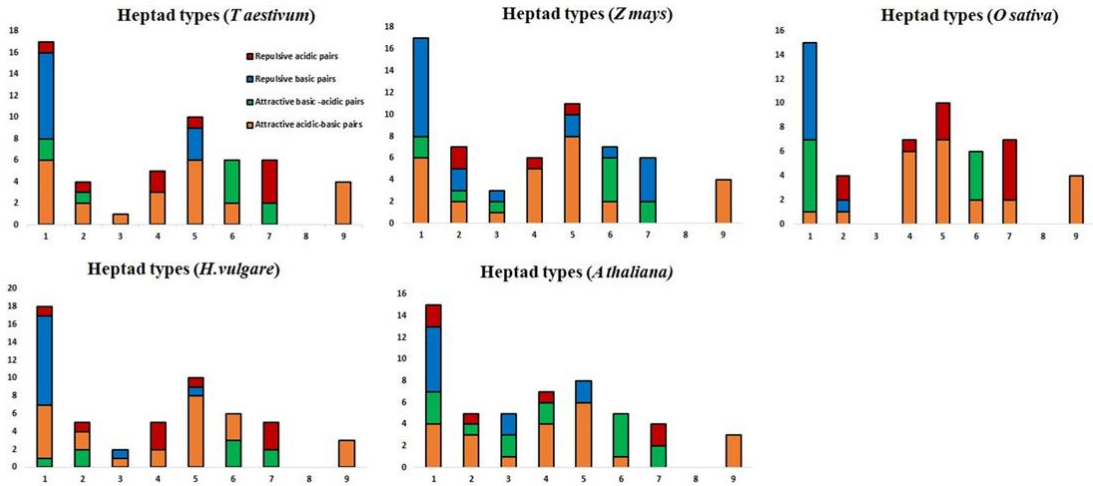
Heptad types (T aestivum)
Repulsive acidic pairs
Repulsive basic pairs
Attractive basic -acidic pairs
Attractive acidic-basic pairs
Heptad types (Z mays)
Heptad types (O sativa)
Heptad types (H.vulgare)
Heptad types (A thaliana)

722

723 **Figure 3 Features of 'a', 'd'. 'e' and 'g' positions in heptads of TabZIPs (A)** Pie chart representing
724 the frequency of occurrence of amino acids in all the *a,d,e and g* positions of heptads in the leucine
725 zipper in *T. aestivum* bZIP family (B) Histograms presenting the dimerization details deduced solely
726 from the presence of N residue at 'a' position in the leucine zipper region of *T. aestivum* and other
727 reference species such as *H. sapiens, A. thaliana, O. sativa, Z. mays* and *H. vulgare*. **(C)** Histogram
728 showing the frequency of attractive or repulsive g↔e′ pairs per heptad for bZIP proteins in bZIP
729 domains of T aestivum, Z mays, O sativa, H vulgare and A thaliana

730

731

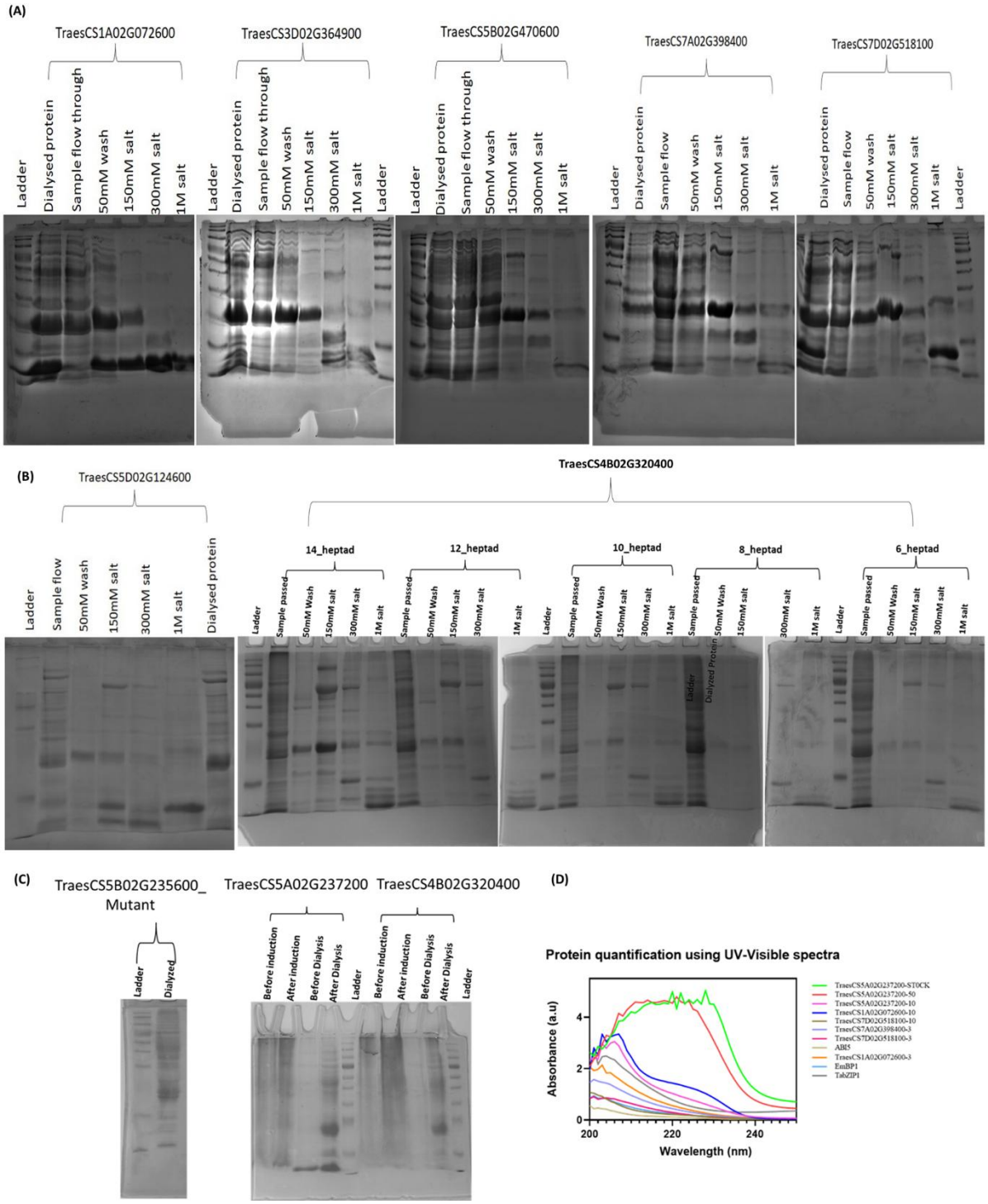

Figure 4 Protein expression of candidate TabZIPs: In panel (A-C) SDS PAGE of expressed TabZIP recombinant proteins in the E-coli bacterial system: TraesCS1A02G072600, TraesCS3D02G364900 (ABI5), TraesCS5B02G470600 (EmBP1), TraesCS7A02G0398400, TraesCS7D02G518100, TraesCS5D02G124600 (TabZIP1), TraesCS5A02G237200, TraesCS5B02G235600 (mutant homeolog), and TraesCS4B02G320400, proteins loaded in the gels following the sequence of

expression steps such as Dialysed protein, sample passed through the heparine sepharose column, 50Mm salt wash, 150 mM salt, 300Mm salt and 1M salt elution step for each protein (D) The HPLC-purified proteins were quantified using UV-Visible spectroscopy to measure the concentration for CD and MALDI-TOF MS.

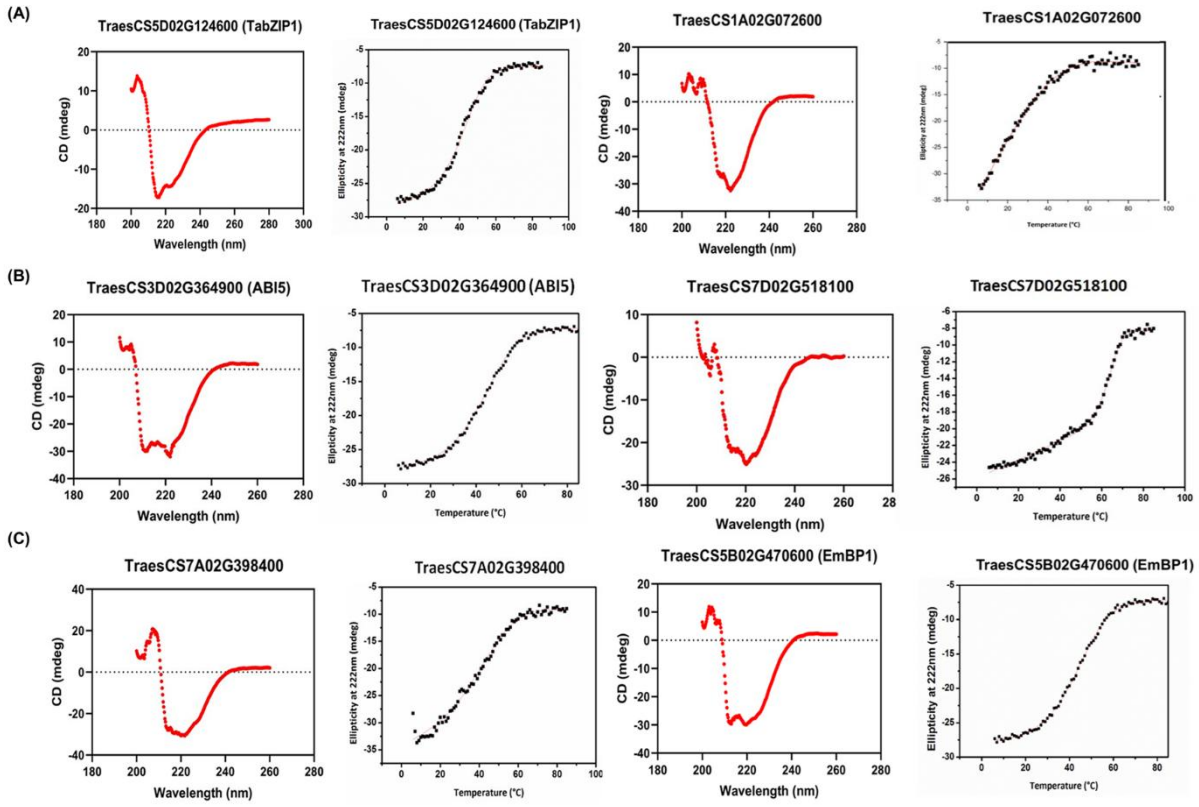

Figure 5 CD wavelength scan and thermal stability analysis of candidate TabZIP proteins. Wavelength scan of bZIP proteins show minima at 222nm and 208 nm, an indicator of alpha helices (red panels). CD thermal denaturation profiles of TabZIPs in 2µM concentration (black panels). The helical content decreased as the temperature was raised from 6-85°C.

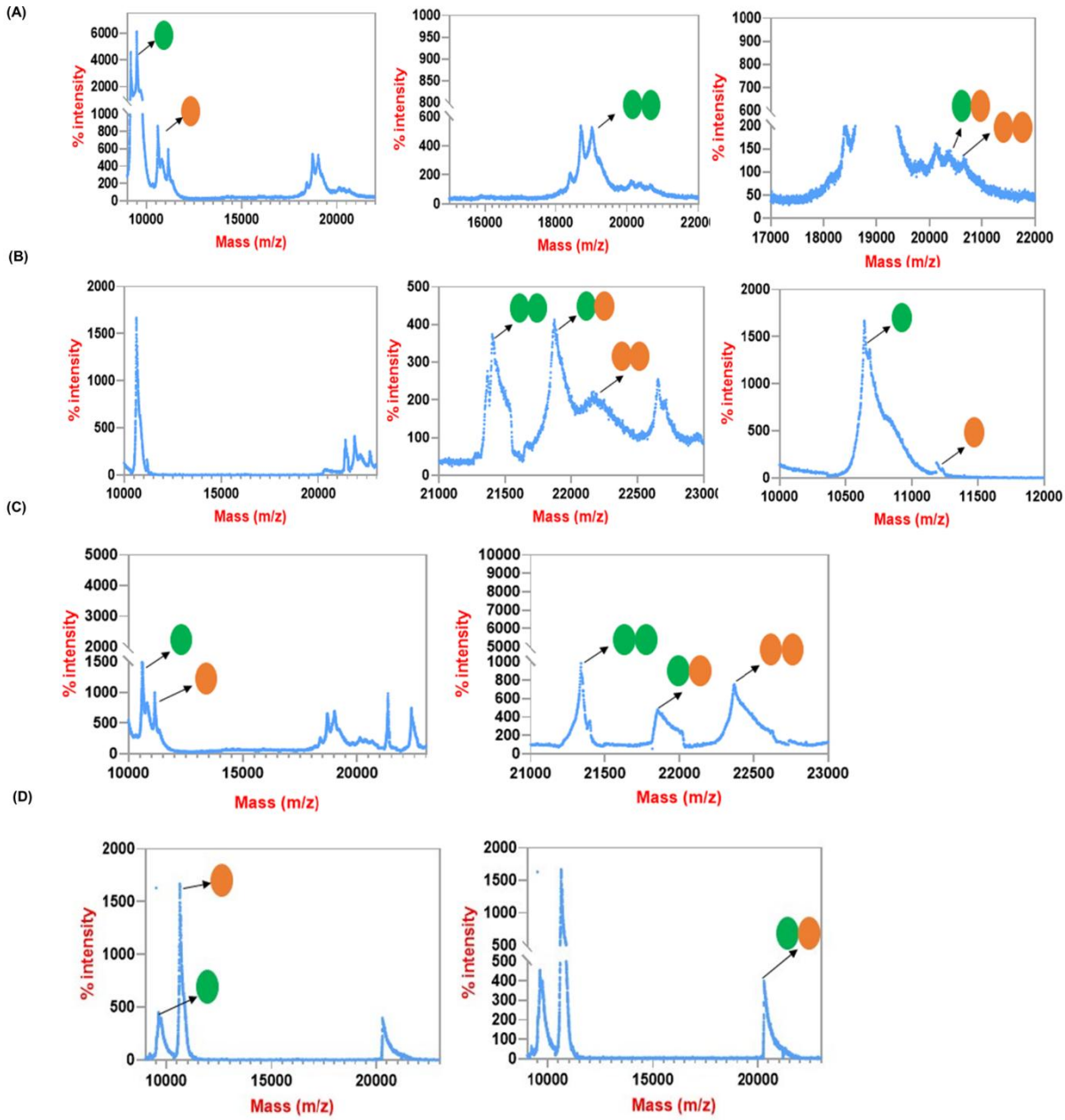

Figure 6 MALDI-TOF mass spectra of candidate TabZIP proteins (A)TraesCS7A02G398400 and TraesCS3D02G364900 (ABI5) in combination with TraesCS1A02G072600, showing both the monomeric peaks (For better understanding peaks have been labelled with circle shapes; single green or orange coloured) and homo- (two shapes with same colour) and heterodimer (two shapes together with different colours) peaks. (B) MALDI-TOF mass spectra TraesCS1A02G072600 and TraesCS5B02G470600 (EmBP1) showing both the monomeric and dimeric peaks. (C) MALDI-TOF mass spectra of TraesCS5B02G470600 (EmBP1) and TraesCS3D02G364900 (ABI5) showing both the monomeric peaks, homo- and heterodimer peaks. (D) MALDI-TOF mass spectra TraesCS1A02G072600 and TraesCS7A02G398400 showing the monomeric peaks and both the homo- and heterodimeric peaks.

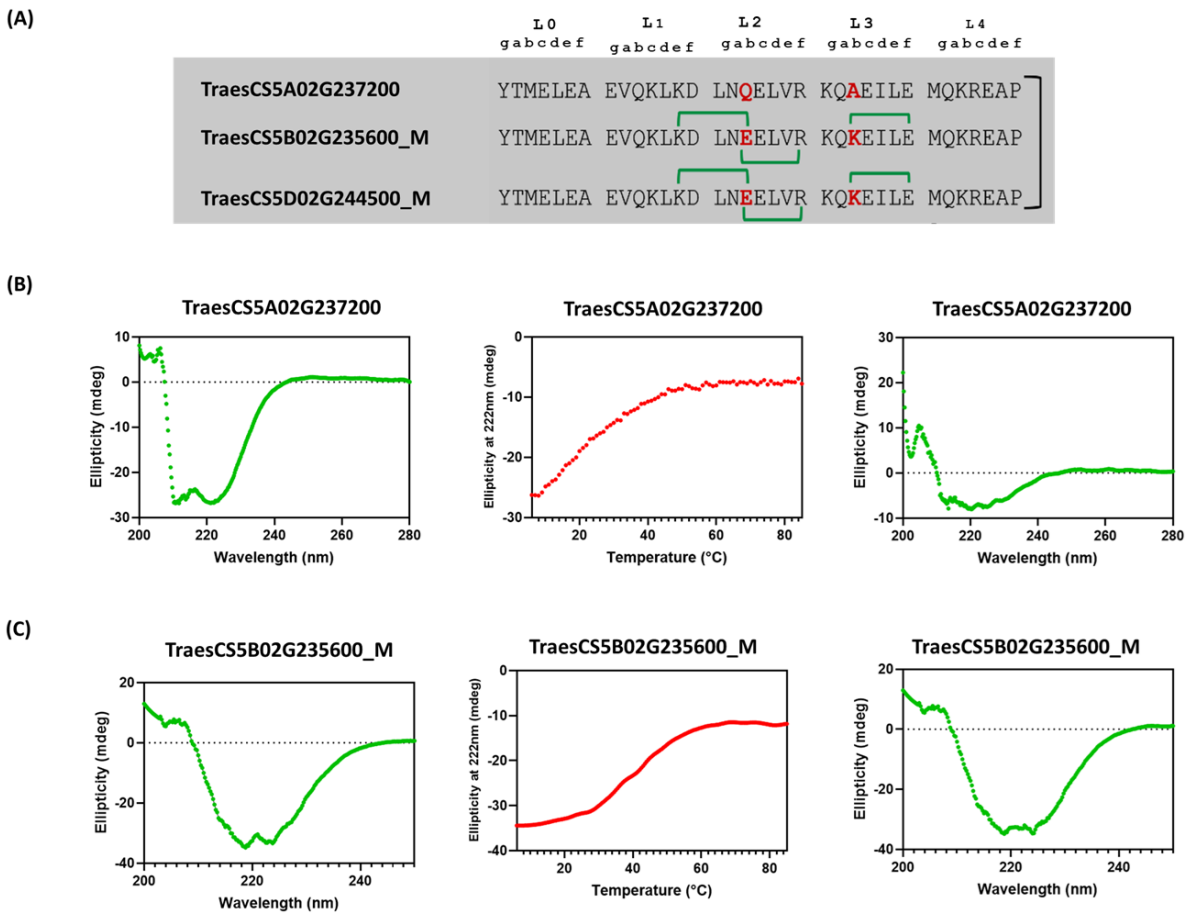

Figure 7 CD wavelength scan and thermal stability analysis of TabZIP TraesCS5A02G237200 and its mutants (A) Protein sequence alignment of the TraesCS5A02G237200 with its homeologs TraesCS5B02G235600 and TraesCS5D02G244500. (B) and (C) Wavelength scan of bZIP proteins show minima at 222nm and 208 nm, an indicator of alpha helices (left green panels). CD thermal denaturation profiles of TabZIPs in 2µM concentration (red panels). The helical content decreased as the temperature was raised from 6-85°C. Reversibility check was performed by re-scanning the wavelength immediately after the thermal denaturation scan, once the sample had cooled to 6°C (right green panels)

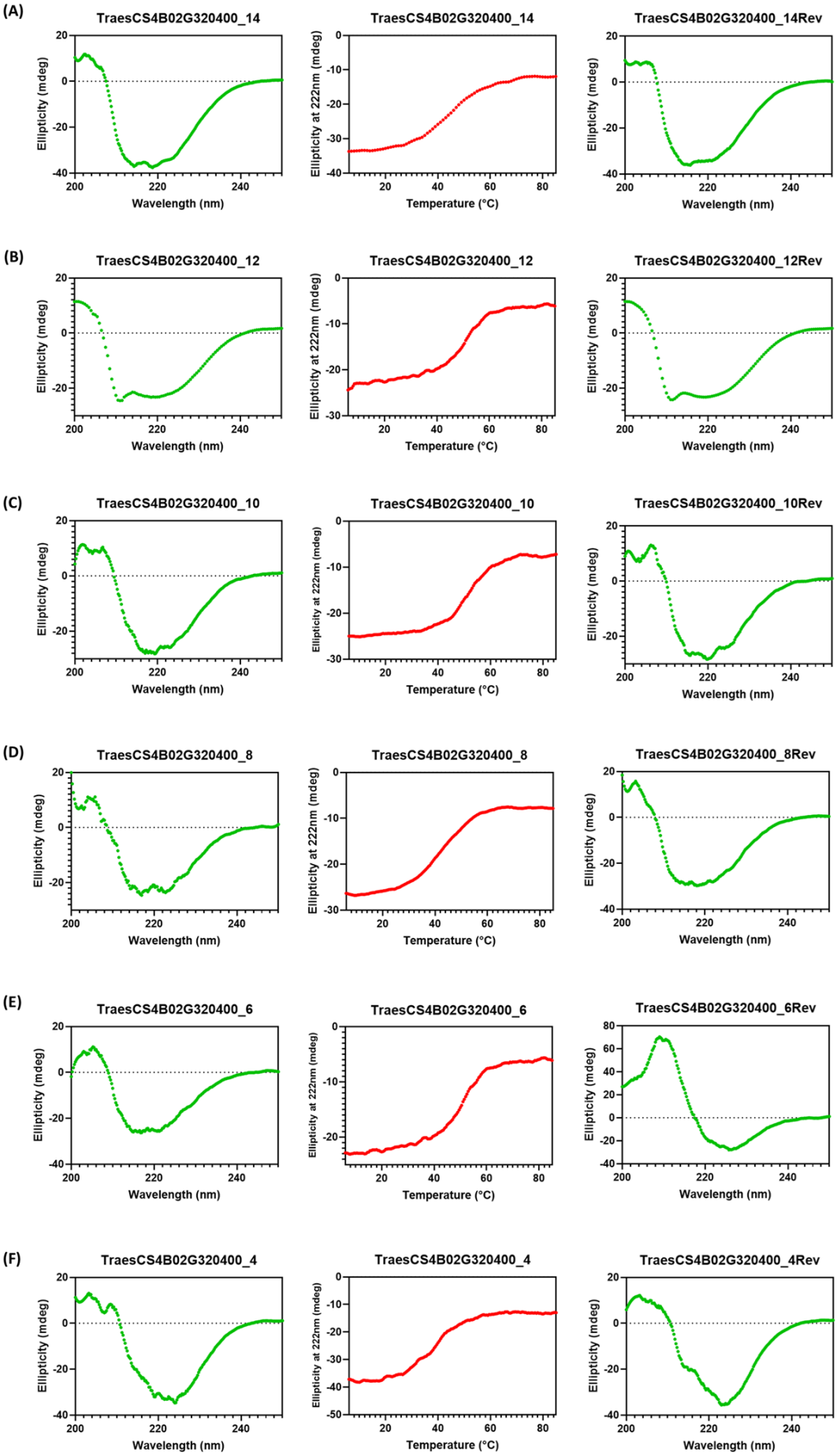
(A)
TraesCS4B02G320400_14
Ellipticity (mdeg)
Wavelength (nm)
TraesCS4B02G320400_14
Ellipticity at 222nm (mdeg)
Temperature (°C)
TraesCS4B02G320400_14Rev
Ellipticity (mdeg)
Wavelength (nm)
(B)
TraesCS4B02G320400_12
Ellipticity (mdeg)
Wavelength (nm)
TraesCS4B02G320400_12
Ellipticity at 222nm (mdeg)
Temperature (°C)
TraesCS4B02G320400_12Rev
Ellipticity (mdeg)
Wavelength (nm)
(C)
TraesCS4B02G320400_10
Ellipticity (mdeg)
Wavelength (nm)
TraesCS4B02G320400_10
Ellipticity at 222nm (mdeg)
Temperature (°C)
TraesCS4B02G320400_10Rev
Ellipticity (mdeg)
Wavelength (nm)
(D)
TraesCS4B02G320400_8
Ellipticity (mdeg)
Wavelength (nm)
TraesCS4B02G320400_8
Ellipticity at 222nm (mdeg)
Temperature (°C)
TraesCS4B02G320400_8Rev
Ellipticity (mdeg)
Wavelength (nm)
(E)
TraesCS4B02G320400_6
Ellipticity (mdeg)
Wavelength (nm)
TraesCS4B02G320400_6
Ellipticity at 222nm (mdeg)
Temperature (°C)
TraesCS4B02G320400_6Rev
Ellipticity (mdeg)
Wavelength (nm)
(F)
TraesCS4B02G320400_4
Ellipticity (mdeg)
Wavelength (nm)
TraesCS4B02G320400_4
Ellipticity at 222nm (mdeg)
Temperature (°C)
TraesCS4B02G320400_4Rev
Ellipticity (mdeg)
Wavelength (nm)

770

771 **Figure 8 CD wavelength scan and thermal stability analysis of TabZIP TraesCS4B02G320400**
772 **and its length variants** (A-F) Wavelength scan of TraesCS4B02G320400 with all length variants,
773 ranging from 4 to 14 heptad repeats, denoted as _4, _6, _8, _10, _12, and _14 heptad lengths, showing
774 minima at 222nm and 208 nm, an indicator of alpha helices (left green panels). CD thermal denaturation
775 profiles of TabZIPs in 2μM concentration (red panels). The helical content decreased as the temperature
776 was raised from 6-85°C. Reversibility check was performed by re-scanning the wavelength immediately
777 after the thermal denaturation scan, once the sample had cooled to 6°C (right green panels)
778

Protein_id	T_m[a], °C	ΔH_m[b], kcal/mol	ΔG_D[c], kcal/mol	Mass (monoisotopic)
TraesCS5B02G470600 (EmBP1)	43	-38	-8.9	11183
TraesCS5D02G124600 (TabZIP1)	43.2	-45	-9.1	12644
TraesCS3D02G364900 (ABI5)	43.1	-37	-8.9	10669
TraesCS7A02G398400	42.5	-32	-8.8	10700
TraesCS1A02G072600	36.6	-18	-8.2	9639
TraesCS7D02G518100	64	-87	-9.5	10653

Table 1 Thermodynamic parameters of candidate TabZIPs

[a]T_m is the midpoint of thermal denaturation. Error in the T_m values of three independent measurements was ≤0.5 °C.

[b] ΔH_m is the enthalpy change at T_m. Values are the mean of three independent measurements and represent ±standard error.

[c]ΔG_D are the values of the free energy change of dimer formation at 25° C and were calculated using the values of ΔHm at corresponding Tm and a ΔCp value of -1.2 ± 0.13 kcal/ mol/ dimer/ K.